Clinical Biomechanics 102 (2023) 105893

Contents lists available at ScienceDirect

Clinical Biomechanics

journal homepage: www.elsevier.com/locate/clinbiomech

Effect of a new transpedicular vertebral device for the treatment or prevention of vertebral compression fractures: A finite element study

Ridha Hambli [a,*], Reade De Leacy [b], Cécile Vienney [c]

[a] Univ. Orléans, Univ. Tours, INSA CVL, LaMé, Orléans 45000, France
[b] Neurosurgery, Icahn School of Medicine at Mount Sinai, New York, NY, USA
[c] Hyprevention, Research and Development, Pessac, France

ARTICLE INFO

Keywords:
Lumbar spine
Vertebral compression fractures
V-STRUT© implant
Restoration
Finite element

ABSTRACT

Background: A finite element study was performed to investigate the biomechanical performance of a novel transpedicular implant (V-STRUT©, Hyprevention, France) made of PEEK (polyetheretherketone) material in terms of strengthening the osteoporotic vertebra and the thoraco-lumbar spine.
The objective was to assess numerically the efficacy of the implant to reduce the stress distribution within bone and absorb part of the stress by the implant thanks to its optimized material selection close to that of normal bone.
Methods: A numerical model was generated based on a scan of an osteoporotic patient. The model is composed of three consecutive vertebrae and intervertebral discs. A heterogeneous distribution of bone material properties was assigned to the bone.
In order to investigate the rationale of the device material selection, three FE models were developed (i) without the device to serve a reference model, (ii) with device made in Titanium material and (iii) with device made in PEEK material.
Stiffness and stress distribution within the spine segment were computed and compared in order to assess the implants' performances.
Findings: The results obtained by the simulations indicated that the novel transpedicular implant made of PEEK material provided support to the superior vertebral endplate, restored the thoraco-lumbar spine segment stiffness and reduced the stress applied to the vertebrae under the compressive load.
Interpretation: Implant geometry in combination with its material properties are very important factors to restore vertebral strength and stiffness and limiting the risk of fracture at the same vertebra or adjacent ones.

1. Introduction

With aging, bone quality decreases due to osteoporosis, increasing the risk of vertebral compression fractures (VCFs) (Melton III, 1997; Bow et al., 2012; Balasubramanian et al., 2019). The VCF incidence rates in Europe and the USA are very similar, with about 570 per 100,000 person-years for men and 1070 per 100,000 person-years for women (Francis et al., 2004). In Asia, the VCF incidence rate is 194 per 100,000 person-years for men and 508 per 100,000 person-years for women (Bow et al., 2012).

The prevalence of this condition increases with age, reaching 40% by age 80. Consequently, non-surgical treatment may lead to a twofold risk of future fractures (22%) compared to treated vertebral procedures (11%) (Papanastassiou et al., 2014). The main current therapeutic options available on the market are vertebroplasty, expandable implantable devices, including balloon kyphoplasty and spinal fusion surgery. Generaly, Vertebroplasty and kyphoplasty are used for stable but painful VCFs and spinal fusion is used in case of unstable fractures.

Vertebroplasty consists of a bone cement injection into the fractured vertebral body under pressure with the goal of stabilizing the fracture (Zhang et al., 2017). It is the current gold standard for surgical treatment of VCFs despite the higher cement leakage rates often associated with this technique (Papanastassiou et al., 2014).

Kyphoplasty and expandable implants such as Kiva® (IZI Medical, USA) or SpineJack® (STRYKER, France) are used to provide vertebral height restoration before cement injection. However, several clinical

* Corresponding author at: Univ. Orléans, Univ. Tours, INSA CVL, LaMé, 8 rue Léonard de Vinci, Orléans 45000, France.
E-mail address: ridha.hambli@univ-orleans.fr (R. Hambli).

https://doi.org/10.1016/j.clinbiomech.2023.105893
Received 24 June 2022; Accepted 10 January 2023
Available online 14 January 2023
0268-0033/© 2023 Published by Elsevier Ltd.

and biomechanical studies have shown that balloon kyphoplasty treatments generate a height loss after deploying the balloons (Verlaan et al., 2005; Voggenreiter, 2005). In two studies performed by Korovessis et al. (2013) and Tutton et al. (2015), the authors compared the performance of balloon kyphoplasty and Kiva® devices. The results showed that both techniques restored vertebral body height similarly in the short term, but that only Kiva® restored vertebral body wedge deformity with a lower rate of leakage.

Cianfoni et al. (2019) developed a novel percutaneous stent screw–assisted internal fixation (SAIF) device to restore and stabilize vertebral body fractures in severe osteoporotic and neoplastic cases. The technique uses two vertebral body stents and percutaneous cannulated and fenestrated pedicular screws, through which cement is injected inside the expanded stents to fill the stents and the vertebral body. Moreover, in a recent retrospective study performed by Venier et al. (2019), the authors assessed the results of armed kyphoplasty using the SAIF Technique or SpineJack® in traumatic, osteoporotic, and neoplastic burst fractures on 53 subjects with respect to vertebral body height restoration and correction of posterior wall retropulsion. The authors concluded that the SpineJack® device is suited for use in patients when bone mass is preserved, especially in young patients with traumatic fractures. Furthermore, the authors recommended use of the SAIF technique for vertebral fractures associated with severe osteoporosis and a high level of vertebral body fragmentation in order to restore stability and axial-load capability. However, the cannulated screw used in the SAIF technique is made of Ti material, which is stiffer than the bone material and hence, it may increase the whole stiffness of the treated vertebra and the lumbar spine segment, increasing the risk of adjacent fractures (Wong and McGirt, 2013).

Spinal fusion surgery is sometimes used in order to connect two or more vertebrae together in the correct position and to eliminate the motion between the vertebrae to eliminate pain. However, this technique also prevents the natural movement of the fused vertebrae, which in turn, limits the patient's movements and increases the stress on the surrounding vertebrae, increasing their risk of fracture and adjacent segment disc disease and degeneration.

To improve VCF treatment, a new surgical device made of PEEK material that is anchored in the pedicles in a minimally invasive procedure has been developed (V-STRUT©, Hyprevention, France) (Fig. 1-a).

Two implants, made of PEEK polymer (PEEK Optima® developed by INVIBIO), are inserted in the vertebral body through the pedicles and combined with the injection of PMMA bone cement and then these will stay in situ (Fig. 1-b).

The transpedicular implantation aims to share load between the anterior and posterior column with the aim of reducing stress in the posterior column, to restore vertebral strength, stabilize the fractured vertebra and prevent the progression of postoperative fractures. The combination of the implant geometry and the choice of material allows an optimal restoration of the treated thoraco-lumbar spine function to a state close to that of a healthy one.

Finite Element (FE) studies have been applied successfully in the field of bone biomechanics especially in the prediction of vertebral and spinal behavior under a variety of conditions (Dreischarf et al., 2014; Sivasankari and Balasubramanian, 2021; Wagnac et al., 2012), vertebral implants (Barbera et al., 2019; Imai et al., 2006; Jhong et al., 2022), assessment of the fixation stability of vertebral implants (Liebschner et al., 2003; Wu et al., 2019), vertebral failure risk evaluation (Groenen et al., 2018) and to investigate the effects of vertebroplasty (Buckley et al., 2007; Chevalier et al., 2008; Dall'Ara et al., 2012). Moreover, FE modeling gives more promising results with a reduced computational time and costs due to the complexity and difficulty of performing in-vitro and in-vivo experiments.

The objective of the current study was to assess numerically the efficacy of the V-STRUT© device alone to restore a lumbar spine segment stiffness, to redistribute the load applied to the treated vertebra, to reduce the stress distribution within bone and to absorb part of the stress by the implant thanks to its design and optimized material selection (PEEK) close to that of normal bone. The cement was not modeled in the current study in order to focus on the role of the implant alone.

2. Methods

In order to better represent the thoraco-lumbar spine response and simulate a more physiological loading condition, in the current work, a CT based FE model was generated composed of three functional spinal units (FSU). In these conditions, the middle vertebra is loaded via two intervertebral discs, thereby transferring load in a realistic way (Fig. 2). Joint facet representations in the model were obtained from the CT scan and the related segmentation procedure. However, it was difficult to identify precisely the facet cartilage in the CT scan and the surrounding ligaments.

The modeling approach consists of three steps: (i) Performing image processing to generate the FE model from the DICOM scans, (ii) inserting the V-STRUT© device CAD model into the middle vertebra as specified by the manufacturer's surgical technique and (iii) simulating the response of the spine/implant model under applied compressive stress.

The approach used here consists in predicting in a first stage the response of the FSU alone without implants and then predicting in a second stage the response of the same FSU with inserted implants for

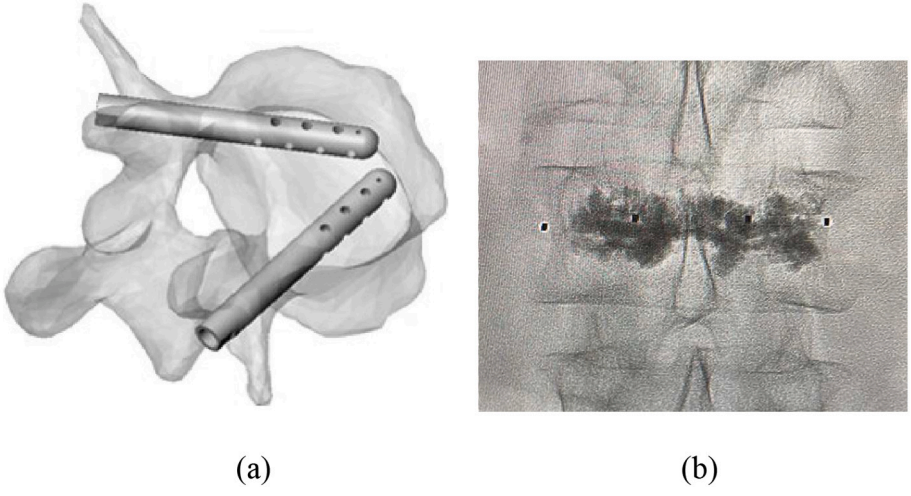

Fig. 1. (a) Representation of V-STRUT© before cement injection in vertebral body. (b) V-STRUT© with bone cement.

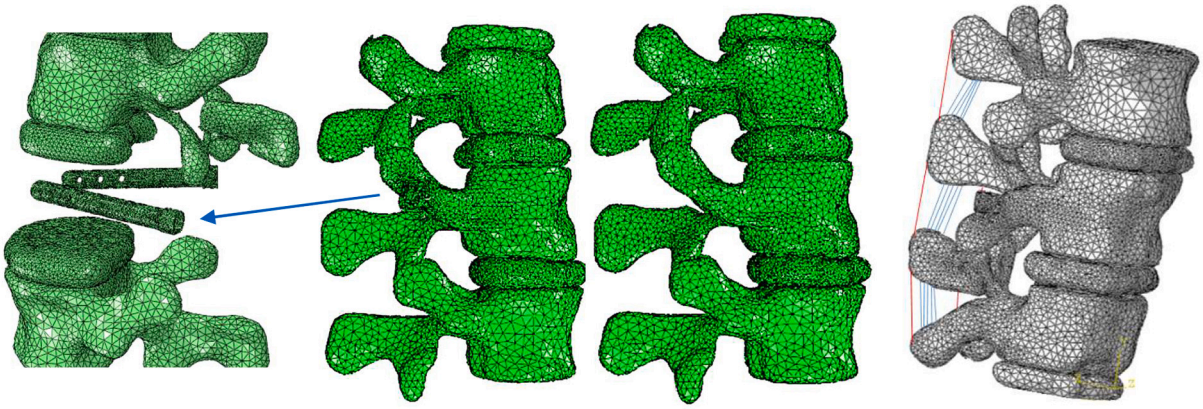

(a) Treated vertebra is removed to show the implants	(b) With the implant	(c) Without the implant	(d) A view of the model showing some ligaments represented by beam elements.

Fig. 2. Finite element model of the thoraco-lumbar spine segment composed of T12, L1 and L2 vertebrae, intervertebral discs and ligaments.

comparison.

V-STRUT© implants made of PEEK material are available in two different diameters (5.5 mm and 6.5 mm). In order to investigate the rationale of the device material selection, two FE models were developed with Titanium (Ti) and PEEK material properties assigned to the V-STRUT© device. Five simulations were then performed to investigate the effect of the two variants of the implant.

Model 1: FSU without the device to serve as a reference model,
Model 2: FSU with inserted device in PEEK material (two diameters),
Model 3: FSU with inserted device in Ti material (two diameters).

Stiffness and stress distribution within the whole FSU and the implants were computed and compared in order to assess the device performance. The compressive stiffness K is expressed by $K = \frac{F}{u}$, where u is the axial compressive displacement of the reference point and F the compressive force.

2.1. Model generation

The FE model was generated based on a CT scan of the thoraco-lumbar spine of an osteoporotic patient (Female, 69 yo, presenting a treated osteoporotic fracture in L3). The geometry was generated using the software ScanIP (Simpleware, Exeter, UK). The model consists of a FSU composed of three consecutive vertebrae (T12, L1 and L2), three intervertebral discs and spinal ligaments (Fig. 2).

Because of the structural complexity of the vertebrae, each FE model was composed of about 350,500 tetrahedral elements to represent the smooth surface of the spinal bone (Groenen et al., 2018; Ulrich et al., 1998). Frictional contact with a friction coefficient of 0.01 was defined between each vertebra/disc surface (Wan et al., 2022). The facet joints were modeled as a frictionless contact with an initial gap of 0.5 mm (Chen et al., 2003).

It has been shown that the main cause of osteoporotic bone fractures is daily normal load rather than traumatic events (Cannada and Hill, 2014). In the current study therefore, the load transfer was limited to the compressive physiological motions of the spine. The superior vertebra (T12) was loaded with a compressive pressure of 1 MPa representing the case of jogging with hard street shoes (Wilke et al., 1999). Reference node were placed at the center of the vertebral body at the inferior vertebra (L2) for the purposes of applying boundary conditions (Fig. 3-a). The nodes at the end plate of the L2 vertebra were then tied to the reference node with beam elements and the reference point was encastered for the simulations.

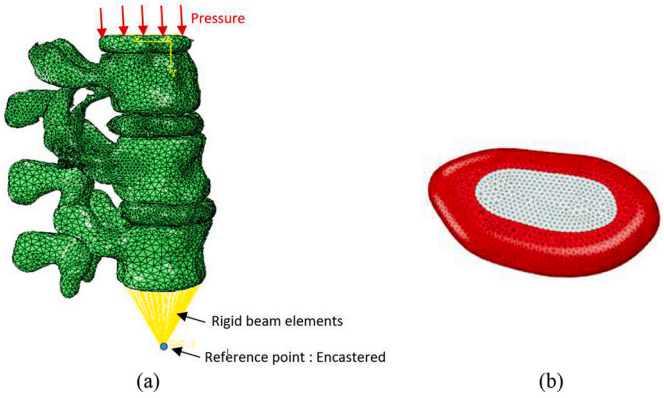

Fig. 3. (a) Loading and boundary conditions applied for the simulations. (b) Intervertebral disc partition into two regions: Annulus fibrosus material (red) and nucleus pulposus material (light grey). (For interpretation of the references to colour in this figure legend, the reader is referred to the web version of this article.)

In the current study, the discs were discretized into two regions (Fig. 3-b) representing the nucleus and the annulus, with the nucleus area constituting approximately 40% of the total disc area (Dreischarf et al., 2014).

2.2. Material properties

Bone was modeled with an elastic linear behavior with a heterogeneous distribution of bone material properties assigned to the vertebrae obtained from the grey scale levels (HU: Hounsfield Unit). The geometry was then imported into the Abaqus code for FE simulations. The intervertebral disc was modeled with nucleus and annulus regions (Fig. 4). Ligaments (Fig. 2) were modeled as linear elastic beams inserted in the assembly with stiffnesses reported from the literature (Neumann et al., 1994; Pintar et al., 1992; Polikeit et al., 2003).

2.2.1. Material properties of bone

The bone density of an element of the vertebral mesh was computed based on the CT value by the following relationship (Morgan et al., 2003:

$$\begin{aligned} \rho &= 0.0 \ (HU \leq 1) \\ \rho &= 0.945\, HU + 1.347.10^{-3} \ (HU > 1) \end{aligned} \quad (1)$$

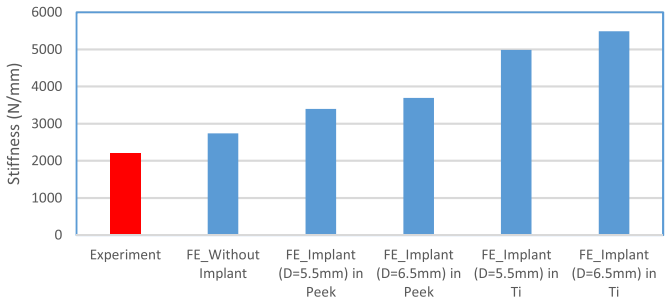

Fig. 4. Predicted stiffnesses for the five FE FSU models. Experimental data for an osteoporotic female for the L12-T2 segment under compressive load are reported in the study of Groenen et al. (2018).

where ρ (g/cm^3) and *HU* denote respectively the bone density and the Hounsfield Unit.

The elastic modulus of each FE was determined based on the relationship between Elastic modulus, E (*MPa*) and the bone density provided by Morgan et al. (2003) as follows:

$$\begin{aligned} E &= 15010\rho^{2.18} \ (\rho \le 0.280) \\ E &= 6850\rho^{1.498} \ (\rho > 0.280) \end{aligned} \tag{2}$$

Poisson's ratio was set to a constant value of: $\nu = 0.3$.

2.2.2. Material properties of intervertebral discs

Typically a hyperelastic Mooney-Rivlin material model is applied for both regions using a strain energy function expressed by (Schmidt et al., 2007; Wilke et al., 1999):

$$W = C10\ (I_1 - 3) + C01\ (I_2 - 3) \tag{3}$$

I_1 and I_2 are the principal strain invariants. $C10$ and $C01$ are material parameters.

The properties for rather degenerated discs were used (Table 1) in the current study (Schmidt et al., 2007).

2.2.3. Material properties of ligaments

The ligaments were modeled as two-noded beam elements according to their anatomical locations and morphologies (Fig. 2), representing the Anterior Longitudinal Ligament (ALL), the Posterior Longitudinal Ligament (PLL), the Supraspinous Ligament (SSL), the Interspinous Ligament (ISL), the Intertransverse Ligament (ITL), Ligament Flavum (LF), and the Facet Capsular Ligament (FCL).

Ligament behavior was described by a linear elastic model with the material properties of each ligament represented by a specific stiffness, given in Table 2 (Neumann et al., 1994; Pintar et al., 1992; Polikeit et al., 2003).

2.2.4. Material properties of the V-STRUT© device

The V-STRUT© device was modeled as a linear elastic isotropic material. The elastic modulus was set respectively to E = 3.6 GPa for PEEK Optima® and E = 110 GPa for Ti (Jhong et al., 2022).

3. Results

In order to validate the FE model, first the predicted stiffness K was compared to published data from experimental and numerical studies (Groenen et al., 2018). In their study, the authors were destructively tested in axial compression twelve two functional spinal units (T6-T8, T9-T11, T12-L2, and L3-L5).

Table 1
Mooney-Rivlin material properties used for the intervertebral discs.

	C10	*C01*
Nucleus	0.18	0.045
Annulus	0.12	0.09

Table 2
Ligament stiffnesses (Neumann et al., 1994; Pintar et al., 1992; Polikeit et al., 2003).

Ligament	Stiffness (N/mm)
Anterior Longitudinal (ALL)	210
Posterior Longitudinal (PLL)	20.4
Supraspinous Ligament (SSL)	23.7
Interspinous Ligament (ISL)	11.5
Intertransverse Ligament (ITL)	50
Ligament Flavum (LF)	27.2
Facet Capsular Ligament (FCL)	33.9

Fig. 4 shows the different predicted FSU stiffnesses.

The computed stiffness for the reference FSU model (without implant) was 2736 N/mm. The average measured compressive stiffness is about 2206 N/mm for an osteoporotic female (Groenen et al., 2018). Although the thoraco-lumbar spine model investigated here was different from that used in previous studies, good agreement was obtained between the predicted results and published experimental ones measured for an osteoporotic female for the L12-T2 segment under compressive load reported in the study by (Groenen et al., 2018). These results indicate that the presented model can be considered as being validated for compression.

An example of the equivalent (von Mises) stress applied to the reference FSU for Ti and PEEK models (diameter = 5.5 mm) is depicted in Fig. 5.

It can be seen that the minimum stress on each vertebra occurs with model 2 when a PEEK implant is used compared to model 1 with no implant. When a Ti device is used, the maximum stress is localized in the vertebra immediately above the treated one. The disc is the main deformable part of the spine under compressive load due to its low elastic properties combined with its high absorbing capacity. Therefore, Ti material increased the stiffness of the treated vertebra, thereby reducing the whole FSU compliance and generating a concentration of stress on the upper vertebra.

On Fig. 6 is plotted the stress distribution generated by the bone/implants contact applied to the implants. The simulations showed that in the case of Ti material, the maximum stress is about 80 MPa and in the case of PEEK material, the maximum stress value do not exceed 10 MPa. For both materials, the V-STRUT© implant is subjected to an elastic stress behavior do not exceeding the yield stresses for both material (110 MPa for PEEK and starting from 260 MPa for Ti depending on the alloy composition).

The results showed that the stress is higher for the implant in Ti compared to the one in PEEK. The deformation level of the implant is lower for Ti (Fig. 7) but as the rigidity of Ti (E = 110 GPa) is about 30 times higher than that of PEEK (E = 3.6 GPa), the Ti implants are subjected to a higher level of stress.

The FE simulations indicated that the V-STRUT© implant undergoes an elastic reversible bending during the compressive load (Fig. 7) (indicating that the device absorbs part of the applied load and hence, reduces the stress applied to the osteoporotic vertebra (Fig. 6).

A cut view of the treated vertebra showing the stress contour at the bone/implant interface (the implant has been removed from the view to show the contour at the interface) (Fig. 8) indicates that the trabecular bone at the interface is subjected to a higher stress level with a stress concentration at the end of the implant. When using PEEK material, the stress level is fivefold lower.

The stress at the bone/implant interface is higher in the case of Ti compared to PEEK. This can be explained by the difference in rigidity between the bone and the device which generates a compliant deformation for the PEEK material and a stiff one for the Ti.

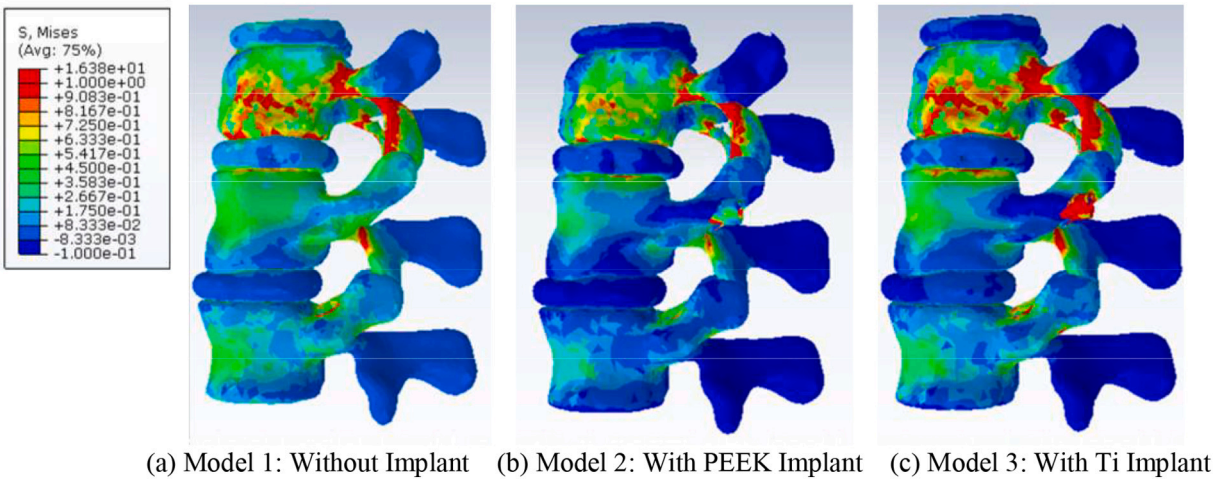

Fig. 5. Distribution of the equivalent stress (von Mises) within the FSU model.

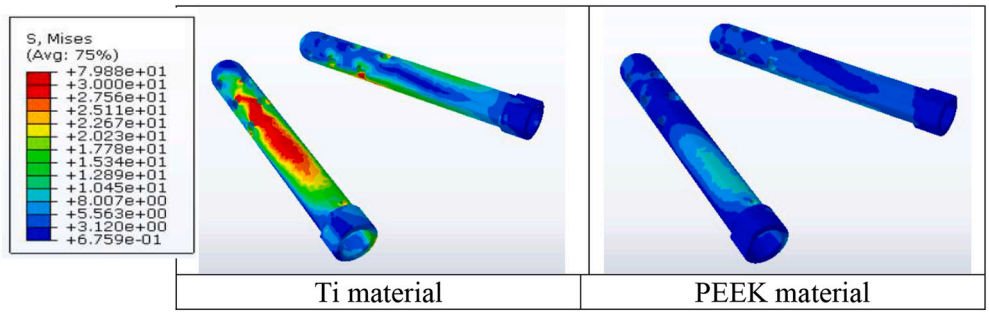

Fig. 6. Contact stress distribution applied to the implant.

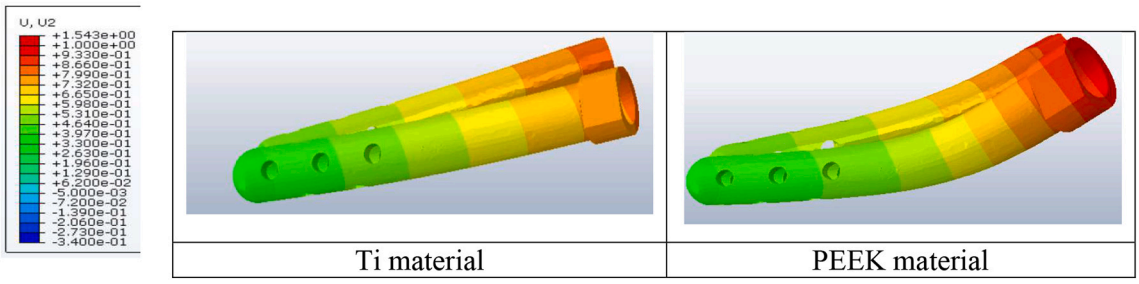

Fig. 7. Distribution of the vertical displacement level showing the bending of the implants (the plot is amplified by a factor of 30 for a better view).

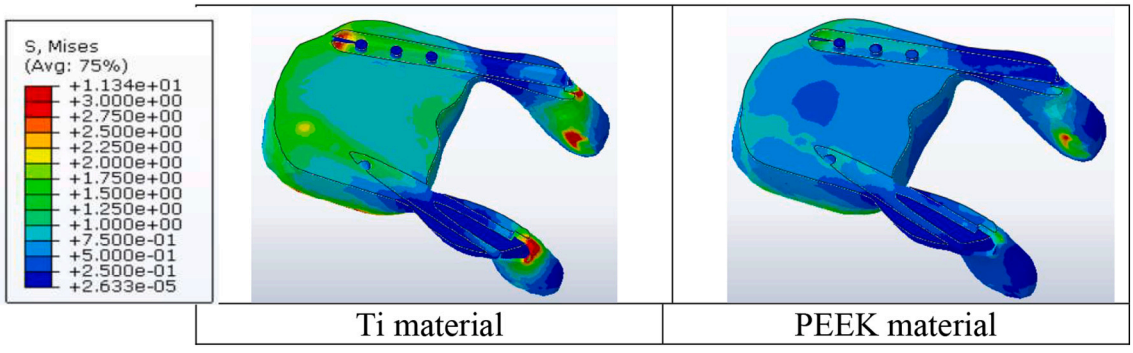

Fig. 8. Contact stress distribution applied to the treated vertebra.

4. Discussion

FSU stiffness (Fig. 4) was increased after V-STRUT© implantation compared to the same model without the implant. The predicted compressive stiffness K was clearly higher for the device made of Ti material compared to the one made of PEEK. The mean percentage increases with respect to the initial values were about +30% and + 87% for PEEK and Ti materials respectively. The Ti material is stiffer (E = 110 GPa) than PEEK (E = 3.6 GPa) and hence, tends to increase the stiffness of the treated FSU. This result indicates that when using Ti on osteoporotic vertebrae, the increased stiffness after treatment reduces the load absorption by the device which may increase the risk of adjacent fractures. Indeed, based on clinical observations for osteoporotic patients, the treated vertebra or the adjacent ones could be subjected to new fractures (Fahim et al., 2011; Polikeit et al., 2003).

Results also show that increasing the implant diameter from 5.5 mm to 6.5 mm leads to an increase of about 11% in the FSU stiffness for both PEEK and Ti materials. This result indicates that the implant dimensions can play a role in strengthening the osteoporotic vertebra and the thoraco-lumbar spine. A patient-specific study is required to investigate the dimension effects on spine stabilization. This is beyond the scope of the present work.

The predicted stress distribution showed that the use of the V-STRUT© device made of PEEK makes it possible to distribute part of the applied load to the treated vertebral body and thus reduce the stress of the whole FSU, increasing its resistance to compressive load. This indicates that a device made of Ti material clearly performs less well than one made of PEEK in restoring the FSU function under compressive load.

An important issue related to the biomaterials used for bone organ implants is to ensure that the material selected has a stiffness close to that of the bone. This is important in order to preserve the bone density in regions in contact with the implants. A problem with some stiff implants made of Ti alloys is that they reduce the load transferred to the neighboring vertebrae and discs, a result known as stress shielding. Stress shielding results in loss of bone density, as the bone no longer has to bear much weight (Mbogori et al., 2022). In addition, PEEK material has many other advantages over metal, such as the possibility of monitoring the healing process using imaging methods. Because of their density, metals absorb X-rays and produce artifacts on the radiographic image, whereas PEEK is transparent to X-rays (Mbogori et al., 2022).

The predicted stress distribution applied to the spine (Fig. 6) and at the bone/implant interface (Fig. 8) clearly indicated that V-STRUT© made from PEEK generated an increase in the whole FSU stiffness compared to the non-treated one with a uniform and lower stress value transferred to the bone and the implant compared to the same implant made from Ti. This may have clinical implications in terms of fracture stabilization and reduction or elimination of pain. The clinical pilot study performed on 6 patients by Cornelis et al. (2021) in order to evaluate the V-STRUT© performance showed that the device provided immediate pain relief and function improvement in all patients in terms of mechanical consolidation of vertebral fracture and transferring the axial compression force to the posterior column.

Several clinical and numerical studies showed that vertebral body height loss may occur after vertebral augmentation or balloon kyphoplasty (Cho et al., 2015; Shin et al., 2021; Verlaan et al., 2005; Voggenreiter, 2005). The recent follow up studies by (Balasubramanian et al., 2019; Shin et al., 2021; Tutton et al., 2015) showed that there is a strong correlation between the vertebral body height loss after vertebral surgical treatment and the risk of adjacent vertebral fractures. About 20% of patients are subjected to adjacent fractures after vertebroplasty (Lindsay et al., 2001; Uppin et al., 2003). Approximately 67% of these new fractures occur in the vertebrae adjacent to the treated one (Uppin et al., 2003).

Cho et al. (2015) showed that increasing the stiffness of the treated vertebra increases the risk of adjacent vertebral fractures after vertebroplasty in an osteoporotic FE model. From a biomechanical point of view, the risk of adjacent vertebral fracture is strongly related to the change in mechanical stress applied to the spine that may be generated after treatment combined with the progression of osteoporosis (Han and Jang, 2018; Noriega et al., 2015).

The V-STRUT© implant was designed by combining an optimal selection of material stiffness close to that of bone (PEEK) and an optimal selection of implant dimensions to ensure a balanced redistribution of the stress on the treated vertebra and the bone/implant interfaces, thereby avoiding a highly increased spine segment stiffness and stress concentration. Such a design may contribute to the reduction of fractures in the adjacent vertebral bodies. Further clinical studies are necessary to investigate the performance of the V-STRUT© implant to reduce adjacent fractures. In addition, the implant is embedded in the pedicle, to provide posterior support. The other part of the device, located in the vertebral body, presents lateral perforations that ensure a spatially uniform and homogeneous diffusion of the cement into the treated vertebral body with a reduced pressure level. Such a design is expected to limit the risk of cement leakage.

The current FE study has some limitations. First, the validity of the FSU model was obtained by comparing the predicted compressive stiffness results with experimentally published ones. Although the thoraco-lumbar spine model investigated here was different from that used in previous studies, good agreement was obtained, confirming the validity of the numerical model. Second, the ligaments were represented as one-dimensional beam elements. Nevertheless, such a representation has been used successfully in the past by different authors.

The third limitation concerns the modeling of the cement effects in combination with the implant. In the current study, the focus was on the role of the implant alone. Fourth, further studies and longer observations are necessary to investigate the short and long terms performance of the V-STRUT© implant under different loading modes with different doses of cement.

5. Conclusion

In conclusion, the present FE investigation showed that the novel transpedicular implant (V-STRUT©, Hyprevention, France) made of PEEK (polyetheretherketone) material brought support to the superior vertebral endplate, restored the thoraco-lumbar spine segment stiffness and reduced the stress applied to the vertebrae under the compressive load, thus limiting the risk of fracture at the same vertebra or adjacent ones. The device is also combined with a relatively low volume of PMMA cement, aiming to avoid injecting a stiff mass into the vertebral body, thus limiting the risk of adjacent fractures (Aebi et al., 2018).

Authorship

All authors were fully involved in the conception and design of the study, acquisition, analysis and interpretation of data, drafting or revising the article. All authors have approved the final article.

Funding

This research did not receive any specific grant from funding agencies in the public, commercial, or not-for-profit sectors.

Declaration of Competing Interest

The study was sponsored by Hyprevention.
No conflict of interest.

References

Aebi, M., Maas, C., Pauli, Di, von Treuheim, T., Friedrich, H., Wilke, H.J., 2018. Comparative biomechanical study of a new transpedicular vertebral device and vertebroplasty for the treatment or prevention of vertebral compression fractures. Clin. Biomech. 56, 40–45.

Balasubramanian, A., Zhang, J., Chen, L., Wenkert, D., Daigle, S.G., Grauer, A., Curtis, J. R., 2019. Risk of subsequent fracture after prior fracture among older women. Osteoporos. Int. 30, 79–92.
Barbera, L., Cianfoni, A., Ferrari, A., Distefano, D., Bonaldi, G., Villa, T., 2019. Stent screw-assisted internal fixation (SAIF) of severe lytic spinal metastases: a comparative finite element analysis of the SAIF technique. World Neurosurg. 128, e370–e377.
Bow, C.H., Cheung, E., Cheung, C.L., Xiao, S.M., Loong, C., Soong, C., Tan, K.C., Luckey, M.M., Cauley, J.A., Fujiwara, S., Kung, A.W.C., 2012. Ethnic difference of clinical vertebral fracture risk. Osteoporos. Int. 23, 879–885.
Buckley, J.M., Loo, K., Motherway, J., 2007. Comparison of quantitative computed tomography-based measures in predicting vertebral compressive strength. Bone 40, 767–774.
Cannada, L.K., Hill, B.W., 2014. Osteoporotic hip and spine fractures: a current review. Geriatr. Orthop. Surg. Rehabil. 5 (4), 207–212.
Chen, S.I., Lin, R.M., Chang, C.H., 2003. Biomechanical investigation of pedicle screw-ver tebrae complex: a finite element approach using bonded and contact interface conditions. Med. Eng. Phys. 25 (4), 275–282.
Chevalier, Y., Charlebois, M., Pahr, D., et al., 2008. A patientspecific finite element methodology to predict damage accumulation in vertebral bodies under axial compression, sagittal flexion and combined loads. Comput. Meth. Biomech. Biomed. Eng. 11, 477–487.
Cho, A.R., Cho, S.B., Lee, J.H., Kim, K.H., 2015. Effect of augmentation material stiffness on adjacent vertebrae after osteoporotic vertebroplasty using finite element analysis with different loading methods. Pain Physician. 18 (6), E1101–E1110.
Cianfoni, A., Distefano, D., Isalberti, M., Reinert, M., Scarone, P., Kuhlen, D., Hirsch, J.A., Bonaldi, G., 2019. Stent-screw-assisted internal fixation: the SAIF technique to augment severe osteoporotic and neoplastic vertebral body fractures. J. Neurointerv. Surg. 11 (6), 603–609.
Cornelis, F.H., Barral, M., Le Huec, J.C., Deschamps, F., De Baere, T., Tselikas, L., 2021. Percutaneous transpedicular fixation by PEEK polymer implants combined with cementoplasty for vertebral compression fractures: a pilot study. Cardiovasc. Intervent. Radiol. 44 (4), 642–646.
Dall'Ara, E., Pahr, D., Varga, P., Kainberger, F., Zysset, P., 2012. QCT-based finite element models predict human vertebral strength in vitro significantly better than simulated DEXA. Osteoporos. Int. 23, 563–572.
Dreischarf, M., Zander, T., Shirazi-Adl, A., Puttlitz, C.M., Adam, C.J., Chen, C.S., Goel, V. K., Kiapour, A., Kim, Y.H., Labus, K.M., Little, J.P., Park, W.M., Wang, Y.H., Wilke, H.J., Rohlmann, A., Schmidt, H., 2014. Comparison of eight published static finite element models of the intact lumbar spine: predictive power of models improves when combined together. J. Biomech. 47, 1757–1766.
Fahim, D.K., Sun, K., Tawackoli, W., Mendel, E., Rhines, L.D., Burton, A.W., Kim, D.H., Ehni, B.L., Liebschner, M.A., 2011. Premature adjacent vertebral fracture after vertebroplasty: a biomechanical study. Neurosurgery 69 (3), 733–744.
Francis, R.M., Baillie, S.P., Chuck, A.J., Crook, P.R., Dunn, N., Fordham, J.N., Kelly, C., Rodgers, A., 2004. Acute and long-term management of patients with vertebral fractures. QJM 97 (2), 63–74.
Groenen, K.H.J., Bitter, T., Veluwen, T.C.G., van der Linden, Y.M., Verdonschot, N., Tanck, E., Janssen, D., 2018. Case-specific non-linear finite element models to predict failure behavior in two functional spinal units. J. Orthop. Res. 36 (12), 3208–3218.
Han, S., Jang, I.T., 2018. 2018, analysis of adjacent fractures after two-level percutaneous vertebroplasty: is the intervening vertebral body prone to te-fracture? Asian Spine J. 12, 524–532.
Imai, K., Ohnishi, I., Bessho, M., et al., 2006. Nonlinear finite element model predicts vertebral bone strength and fracture site. Spine (Phila Pa 1976) 31, 1789–1794.
Jhong, G.H., Chung, Y.H., Li, C.T., Che, Y.N., Chang, C.W., Chang, C.H., 2022. Numerical comparison of restored vertebral body height after incomplete burst fracture of the lumbar spine. J. Pers. Med. 12 (2), 253, 10.
Korovessis, P., Vardakastanis, K., Repantis, T., Vitsas, V., 2013. Balloon kyphoplasty versus KIVA vertebral augmentation–comparison of 2 techniques for osteoporotic vertebral body fractures: prospective randomized study. Spine (Phila Pa 1976) 38 (4), 292–299, 15.
Liebschner, M.A., Kopperdahl, D.L., Rosenberg, W.S., et al., 2003. Finite element modeling of the human thoracolumbar spine. Spine (Phila Pa 1976) 28, 559–565.
Lindsay, R., Silverman, S.L., Cooper, C., Hanley, D.A., Barton, I., Broy, S.B., Licata, A., Benhamou, L., Geusens, P., Flowers, K., Stracke, H., Seeman, E., 2001. Risk of new vertebral fracture in the year following a fracture. JAMA. 285 (3), 320–323.
Mbogori, M., Vaish, A., Vaishya, R., Haleem, A., Javaid, J., 2022. Poly-Ether-Ether-Ketone (PEEK) in orthopaedic practice- a current concept review, 1 (1), 3–7.
Melton III, L.J., 1997. Epidemiology of spinal osteoporosis. Spine 22 (24 suppl), 2S–11S.
Morgan, E.F., Bayraktar, H.H., Keaveny, T.M., 2003 Jul. Trabecular bone modulus-density relationships depend on anatomic site. J. Biomech. 36 (7), 897–904.
Neumann, P., Keller, T.S., Ekström, L., Hansson, T., 1994. Effect of strain rate and bone mineral on the structural properties of the human anterior longitudinal ligament. Spine 19, 205–211.
Noriega, D., Maestretti, G., Renaud, C., Francaviglia, N., Ould-Slimane, M., Queinnec, S., Ekkerlein, H., Hassel, F., Gumpert, R., Sabatier, P., Huet, H., Plasencia, M., Theumann, N., Kunsky, A., Krüger, A., 2015. Clinical performance and safety of 108 SpineJack implantations: 1-year results of a prospective multicentre single-arm registry study. Biomed. Res. Int. 173872.
Papanastassiou, I.D., Filis, A., Aghayey, K., Kokkalis, Z.T., Gerochristou, M.A., Vrionis, F., 2014. Adverse prognostic factors and optimal intervention time for kyphoplasty/vertebroplasty in osteoporotic fractures. Biomed. Res. Int. 2014, 925683.
Pintar, F.A., Yoganandan, N., Myers, T., Elhagediab, A., Sances, A., Jr., 1992. Biomechanical properties of human lumbar spine ligaments. J. Biomech. 25, 1351–1356.
Polikeit, A., Nolte, L.P., Ferguson, S.J., 2003. The effect of cement augmentation on the load transfer in an osteoporotic functional spinal unit: finite-element analysis. Spine 28, 991–996.
Schmidt, H., Heuer, F., Drumm, J., Klezl, Z., Claes, L., Wilke, H.J., 2007. Application of a calibration method provides more realistic results for a finite element model of a lumbar spinal segment. Clin. Biomech. 22, 377–384.
Shin, H.K., Park, J.H., Lee, I.G., Park, J.H., Park, J.H., Cho, Y., 2021. A study on the relationship between the rate of vertebral body height loss before balloon kyphoplasty and early adjacent vertebral fracture. J. Back Musculoskelet. Rehabil. 34 (4), 649–656.
Sivasankari, S., Balasubramanian, V., 2021. Influence of occupant collision state parameters on the lumbar spinal injury during frontal crash. J. Adv. Res. 28, 17–26.
Tutton, S.M., Pflugmacher, R., Davidian, M., Beall, D.P., Facchini, F.R., Garfin, S.R., 2015. KAST study: the Kiva system as a vertebral augmentation treatment-A safety and effectiveness trial: A randomized, noninferiority trial comparing the Kiva system with balloon Kyphoplasty in treatment of osteoporotic vertebral compression fractures. Spine (Phila Pa 1976) 40 (12), 865–875, 15.
Ulrich, D., van Rietbergen, B., Weinans, H., Ruegsegger, 1998. Finite element analysis of trabecular bone structure: a comparison of image-based P. meshing techniques. J. Biomech. 31, 1187–1192.
Uppin, A.A., Hirsch, J.A., Centenera, L.V., Pfiefer, B.A., Pazianos, A.G., Choi, I.S., 2003. Occurrence of new vertebral body fracture after percutaneous vertebroplasty in patients with osteoporosis. Radiology. 226 (1), 119–124.
Venier, A., Roccatagliata, L., Isalberti, M., Scarone, P., Kuhlen, D.E., Reinert, M., Bonaldi, G., Hirsch, J.A., Cianfoni, A., 2019 Nov. Armed Kyphoplasty: an indirect Central Canal decompression technique in burst fractures. AJNR Am. J. Neuroradiol. 40 (11), 1965–1972.
Verlaan, J.J., van de Kraats, E.B., Oner, F.C., Van Walsum, T., Niessen, W.J., Dhert, W.J. A., 2005. The reduction of endplate fractures during balloon vertebroplasty: a detailed adiological analysis of the treatment of burst fractures using pedicle screws, balloon vertebroplasty, and calcium phosphate cement. Spine 30 (16), 1840–1845.
Voggenreiter, G., 2005. Balloon kyphoplasty is effective in deformity correction of osteoporotic vertebral compression fractures. Spine 30 (24), 2806–2812.
Wagnac, E., Arnoux, P.J., Garo, A., Aubin, C.E., 2012. Finite element analysis of the influence of loading rate on a model of the full lumbar spine under dynamic loading conditions. Med. Biol. Eng. Comput. 50, 903–915.
Wan, S., Xue, B., Xiong, Y., 2022. Three-dimensional biomechanical finite element analysis of lumbar disc herniation in middle aged and elderly. J. Healthc. Eng. 15 (2022), 7107702.
Wilke, H.J., Neef, P., Caimi, M., Hoogland, T., Claes, L.E., 1999. New in vivo measurements of pressures in the intervertebral disc in daily life. Spine (Phila Pa 1976) 24 (8), 755–762, 15.
Wong, Cyrus C., McGirt, Matthew J., 2013. Vertebral compression fractures: a review of current management and multimodal therapy. J. Multidiscip. Healthc. 6, 205–214.
Wu, T., Meng, Y., Wang, B., Rong, X., Hong, Y., Ding, C., Chen, H., Liu, H., 2019. Biomechanics following skip-level cervical disc arthroplasty versus skip-level cervical discectomy and fusion: a finite element based study. BMC Musculoskelet. Disord. 20, 49.
Zhang, L., Wang, Q., Wang, L., Shen, J., Zhang, Q., Sun, C., 2017. Bone cement distribution in the vertebral body affects chances of recompression after percutaneous vertebroplasty treatment in elderly patients with osteoporotic vertebral compression fractures. Clin. Interv. Aging 12, 431–436.